“Study of Intermetallic Compound Growth and Failure Mechanisms in Long Term Reliability of Silver Bonding Wire”

by

You Cheol Jang*, So Yeon Park*, Hyoung Dong Kim*,
Yeo Chan Ko*, Kyo Wang Koo*, Jae Hak Yee*,
Mi Ri Choi**, Sung Hwan Lim**,
Hyung Giun Kim***,
Nam Kwon Cho****, Il Tae Kang****
* R&D, STATS ChipPAC Korea, Icheon, Republic of Korea
** Department of Advanced Materials Science and Engineering,
Kangwon National University, Republic of Korea
*** Gangwon Regional Division, Korea Institute of Industrial Technology,
Gangneung, Republic of Korea
**** R&D, Heraeus Oriental HiTec Co., Ltd, Incheon, Republic of Korea
youcheol.jang@statschippac.com

Study of Intermetallic Compound Growth and Failure Mechanisms in Long Term Reliability of Silver Bonding Wire

You Cheol Jang[a], So Yeon Park[a], Hyoung Dong Kim[a], Yeo Chan Ko[a], Kyo Wang Koo[a], Mi Ri Choi[b], Hyung Giun Kim[c], Nam Kwon Cho[d], Il Tae Kang[d], Jae Hak Yee[a,*], Sung Hwan Lim[b,*]

[a] R&D, STATSChipPAC Korea, Icheon, Republic of Korea
[b] Department of Advanced Materials Science and Engineering, Kangwon National University, Republic of Korea
[c] Gangwon Regional Division, Korea Institute of Industrial Technology, Gangneung, Republic of Korea
[d] R&D, Heraeus Oriental HiTec Co., Ltd, Incheon, Republic of Korea

youcheol.jang@statschippac.com

Abstract

Silver wires have become a novel bonding material in recent years. But users & field engineers are still divided over the issue of reliability performance including failure mechanism and intermetallic compounds (IMCs) formation. In this study, new type of high purity silver wire with 96Ag-3Pd-1Au alloy (96% Ag) is introduced, and the bonding properties on Al bond pad are evaluated through bondability & reliability test. Reliability tests for wire characterization are high-temperature-storage lifetime test (HTST) and unbiased highly-accelerated stress test (uHAST) with temperature and humidity. Two types of mold compounds are used which have different Cl- ion content. Below 10 ppm of Cl- ion for the green compound and 27 ppm for the normal one. Bondability, IMC formation(Ag_2Al, Ag_3Al) & growth rate are measured for both HTST150'C & 175'C for 2000h and the possible failure mechanism is defined based on the micro-structural characterization from uHAST in which the repetitive oxidation and reduction reactions occur due to the galvanic reaction and the Cl- ions with sufficient moisture and thermal energy, and the reduction reaction of Ag-Al IMCs and Al pad causes to form the micro-crack failure.

Introduction

Wire bonding is the most common and traditional interconnection method for IC packages [1-3]. Although gold wire has many advantages in terms of its workability and stable chemical properties, identifying a low cost bonding material to reduce packaging costs is currently a pressing issue and highlighted activity [4]. In this aspect, from the perspective of its better workability, lower risk of bond pad metal cracking, and similar electrical conductivity and properties to gold wire, silver wire has attracted higher attention of late as a lower cost solution than Cu wire [5-10]. And also, technologies of Pd coating and the doping on Ag bonding wire have been introduced, which improve the efficiency of the fabrication process and the Ag-Al bond reliability [5, 6].

In the initial development stage of Ag-rich wire, 88% (88Ag-8Au-3Pd) Ag bonding wire had been introduced which could improve the properties of the Ag-Al bond reliability [7-10]. Regarding the phases of the Ag-Al IMCs, Ag_5Al, Ag_3Al, Ag_2Al, AgAl and $AgAl_3$ have been reported to have been formed, including the phases via first-principles methods [12-16]. Previously, Guo et al. [17] have reported that $AuAl_2$,

Item	Description
PKG Dimension	19x19 mm, 369LD
Substrate thickness	0.36T
Die size	7.0x6.0 mm
Wire diameter	0.7mils (17.8um), 96% Ag
BPO/BPP	43um / 50um
Mold cap thickness	0.3T

Figure 1. Test package structure

$(Au,Ag)_4Al$, and Ag_2Al are formed in the Au-Ag alloy-Al bond. Kai et al. [18] and Cheng et al. [19] have proposed that Ag_4Al, Ag_3Al and Ag_2Al are formed at the bonding interface in the Ag-Au-Pd alloy-Al bond.

However, the considerable amount of Au addition in the Ag bonding wire may still increase the resistivity and hardness as well as wire cost. Therefore, silver wire market needs advanced type of Ag wire more similar to Au wire properties in terms of wire softness for die to die bonding and a low resistivity for IC / memory device of high power / frequency technology trend. It becomes a promotion of the advent of high silver content wire. The 96% Ag wire (96Ag-1Au-3Pd) has been introduced & confirmed to have good properties akin to 2N gold wire and cost reduction effect as well due to high silver and low gold alloy design. Further evaluation of 96% Ag wire is needed for bondability & reliability. Hence, the present study is carried out to investigate IMC formation and growth between 96% Ag wire and Al pad metallization under thermal reliability conditions and to define the failure mechanisms through the micro-structural characterization.

Experimental

The device has 1.3µm-thick Al pads for this experiment. The package structure is as shown in Figure 1.

0.7mil (17.8µm), 96% Ag bonding wires (AgULTRA, Heraeus Oriental HiTec) were bonded on the thin Al pads and molded using Green and Normal EMCs. The concentration of Cl- ion was below 10 ppm for the Green and was 27 ppm for the Normal EMCs. For the Ag-Al bonding process, an automated bonding machine equipped with a capillary was

978-1-4799-6994-4/14/$31.00 ©2014 IEEE

utilized. The process was conducted to determine the optimum bonding parameters. In the long term reliability test, HTST was carried out at 150°C and 175°C for 0 to 2,000 h. All the specimens were protected from the oxidizing atmosphere by N_2 gas in oven chambers at 175°C during HTST. And uHAST was also carried out at 130°C for 0 and 192 h in 85%RH using the uHAST chamber.

To determine the bondability between the Al pad and the Ag wire, a bond pull test (BPT) and ball shear test (BST) were conducted using a testing machine. And, to evaluate the morphological change and the growth rate of the Ag-Al IMCs during the reliability test, the evolution of IMCs at the bonding interface was observed using optical microscopy (OM) and scanning electron microscopy (SEM).

The specimen was mechanically polished and then ion-polished for fine polishing. To identify the phases in the Ag-Al IMCs and the failure mechanism, SEM analysis was conducted with energy-dispersive X-ray spectroscopy (EDS) and particularly by transmission electron microscopy (TEM).

Results

1. Bondability of Ag-Al bond during HTST

The bond pull strength and the ball shear strength during the HTSTs at 150°C and 175°C are shown in Figure 2 that data of 150°C is higher than that of 175°C because of different IMC growth rate. It means IMC growth rate is higher at 175°C than at 150°C and there is close relationship between Reliability performance and IMC growth rate. Therefore, thermal aging properties at 150°C during HTSTs showed much greater stability than those at 175°C.

Also the ball lifts and low test values during BPT and BST occurred after 1,000 h at 150 °C and after 240 h at 175 °C and they could have different appearance in case of molded units, while gold wire had stable values of BPT and BST until 1000 h at both 150°C and 175°C. Impurities of PCB and moisture in atmosphere might cause the degradation of Ag-Al bonds.

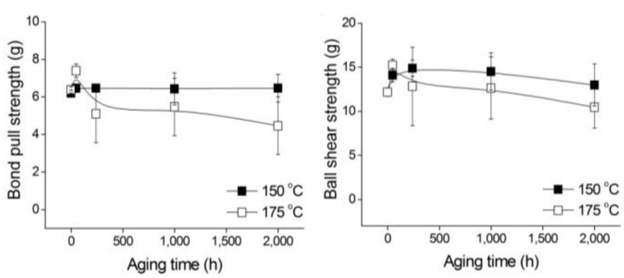

(a) BPT (b) BST

Figure 2. Bondability graph during HTST

2. IMC structure comparison between Au-Al and Ag-Al bond

The sequence of intermetallic phase transformation per aging time under HTST 175°C for both Au-Al and Ag-Al bonds is shown in Figure 3. These are from cross-section of the molded units per aging time.

After HTST at 175 °C for 48 h, the IMC was grown the Ag bonding wire and Al pad by the atomic inter-diffusion of Ag and Al atoms.

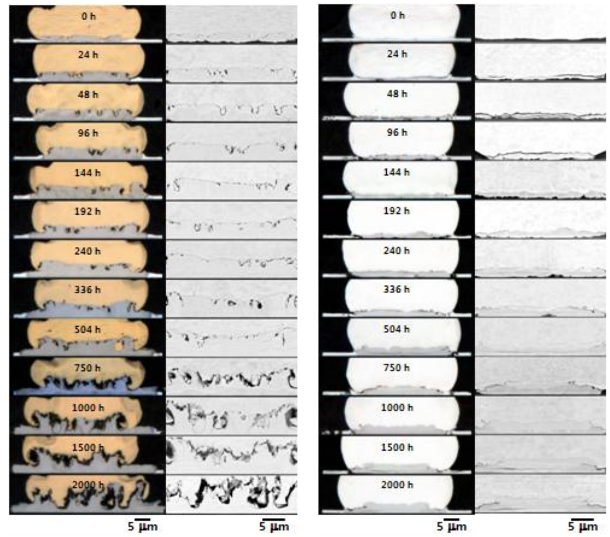

(a) Au-Al bond (b) Ag-Al bond

Figure 3. IMC growth during HTSTs (175°C) aging time

After HTST at 175°C for 240 h, Ag_3Al was detected between Ag_2Al and Ag. A continuous and thin alumina layer, which should generally be split during the bonding process, was found to remain at the bonding interface. After HTST at 175°C for 2,000 h, Ag_3Al and Ag_2Al were considerably grown and the Al pad was also entirely consumed; a large-crack was observed. And, no clustering of alloying Au and Pd elements was observed; these alloying elements were considered to be uniformly distributed even after the HTSTs. It was therefore suggested that the elemental addition of Au and Pd might increase the resistance to oxidation and sulfuration of Ag bonding wire [10]. In the case of Au-Al bond, micro-cracks and kirkendall voids were observed. The IMCs were grown on the Al pad, then the Au_8Al_3 was transformed to Au_4Al. These phases changed as a function of temperature and time. It is indicated in Figure 4.

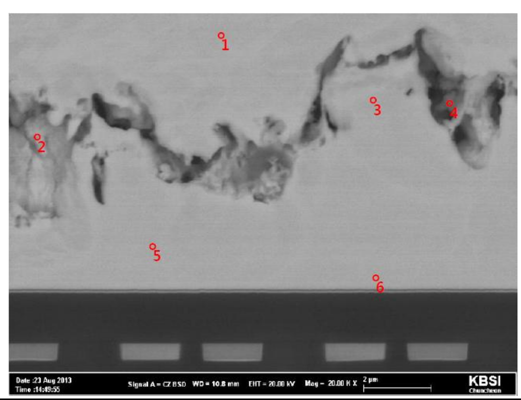

Weight%	Au	Al	Pd	Remark
1	99.40	-	0.60	Au wire
2	92.18	4.83	2.99	Au_8Al_3
3	93.48	4.79	1.73	Au_8Al_3
4	92.75	4.47	2.78	Au_8Al_3
5	94.73	4.73	0.55	Au_8Al_3
6	94.99	5.01	-	Au_8Al_3

Figure 4. IMC phase of Au-Al bond at HTST 1,500h

On the other hand, Figure 5 shows FE-SEM images of the interface of the Ag-Al bonds. The Ag_3Al IMC region is represented by point #2 and Ag_2Al IMC is indicated by point #3 to 6.

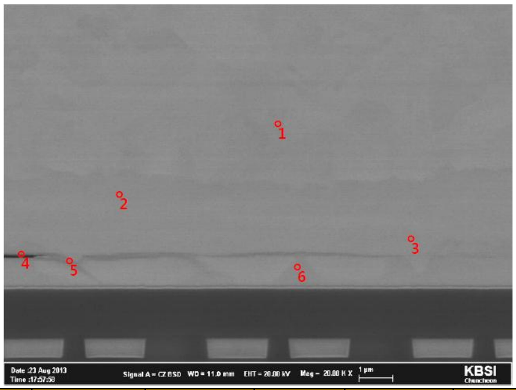

Weight%	Ag	Al	Pd	Au	Remark
1	95.74	-	4.15	0.11	Ag wire
2	87.62	6.84	4.19	1.36	Ag_3Al
3	87.03	9.92	3.05	-	Ag_2Al
4	87.7418	11.67	0.55	-	Ag_2Al
5	90.41	9.59	-	-	Ag_3Al
6	88.00	10.21	-	1.79	Ag_2Al

Figure 5. IMC phases of Ag-Al bond at HTST 1,500h

3. Comparison of IMC growth rate using 2 types of mold compound in the Ag-Al bond

Figure 6 is shown the sequential cross-sectional OM and SEM images of the interface at molded Ag-Al bonds after HTSTs at 150°C and 175°C for 0 to 2,000 hours with the Green and Normal EMCs. No morphological differences in the IMCs growth with Green and Normal EMCs are noted in this figure. The effect of temperature on the thickness of IMCs was clearly observed, such that the thickness of IMCs became much greater as the temperature increased.

- HTST at 150°C -

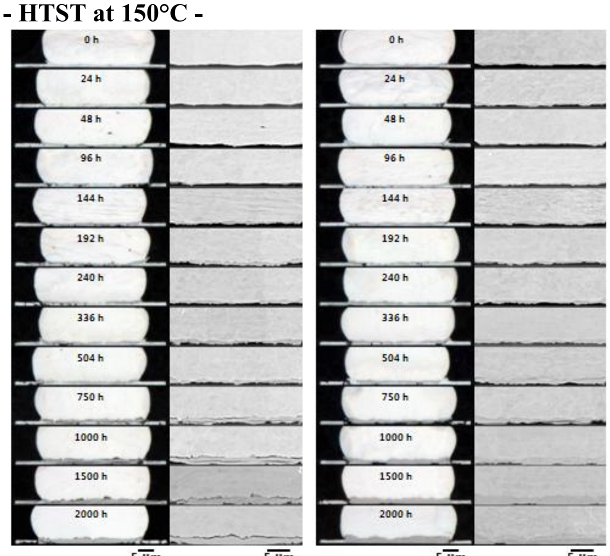

(a) Green EMC (b) Normal EMC

- HTST at 175°C -

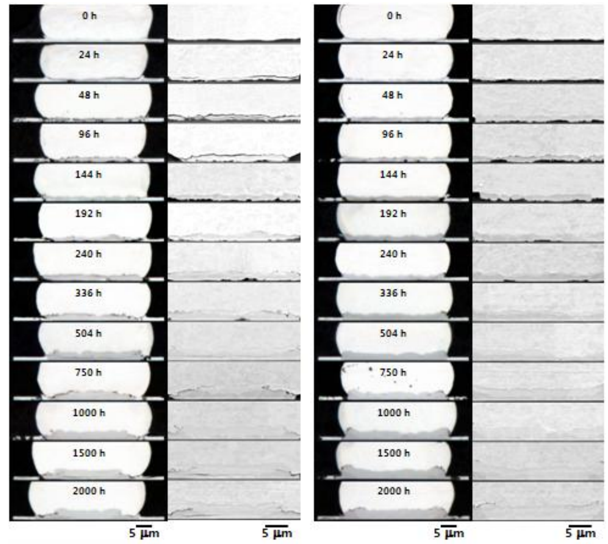

(c) Green EMC (d) Normal EMC

Figure 6. Sequential cross-sectional images for 0 to 2,000 hours in HTSTs at 150°C and 175°C

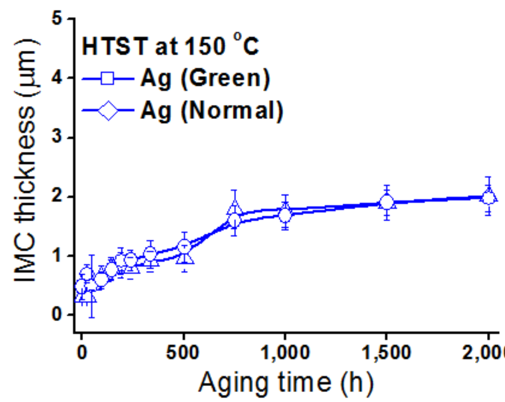

(a) HTSTs at 150°C

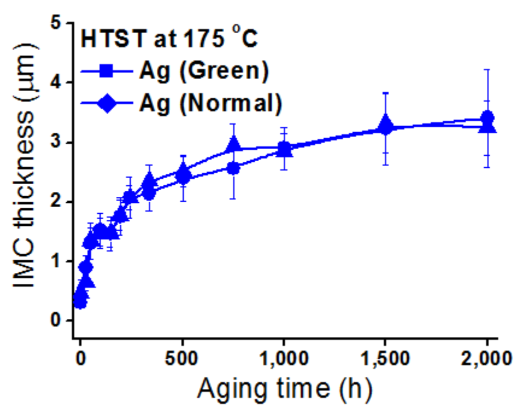

(b) HTSTs at 175°C

Figure 7. Growth of IMC thickness as a function of aging time in Green and Normal EMCs molded Ag-Al bonds.

Figure 7 shows the measured thicknesses values for the Ag-Al bonds in Green and Normal EMCs during HTST at 150°C and 175°C. These figures suggest that the growth rate, D (cm^2/s), follows the equations shown below [11]:

$$x = (Dt)^{1/2}$$

$$D = D_0 \exp\left(-\frac{\Delta Q}{RT}\right)$$

$$\ln D = \left(-\frac{\Delta Q}{R}\right)\left(\frac{1}{T}\right) + \ln D_0$$

where T is the aging temperature (K), x is the IMC thickness (um), t is the aging time (s), R is gas constant, △Q represents activation energy for IMC formation (kcal/mol). The growth rate constants (D) for each condition were calculated from Figure 7 and are summarized in Table 1.

Table 1. Growth rate constants of IMC, in Green and Normal EMC molded Ag-Al bonds during HTST at 150 and 175 °C.

EMC type	Temp. (°C)	*D* (cm^2/s)
Green	150°C	4.46×10^{-15}
	175°C	2.05×10^{-14}
Normal	150°C	3.54×10^{-15}
	175°C	1.25×10^{-14}

4. Failure mechanism in Ag-Al bond during uHAST

Figure 8 shows the cross-sectional FE-SEM image of molded Ag-Al bond after uHAST 192 hours with Green EMC. The unit was not failed at the electrical test but the critical micro-cracks and voids were observed, which were gradually evolved in the IMC layers of both Ag_2Al and Ag_3Al with the uHAST aging time.

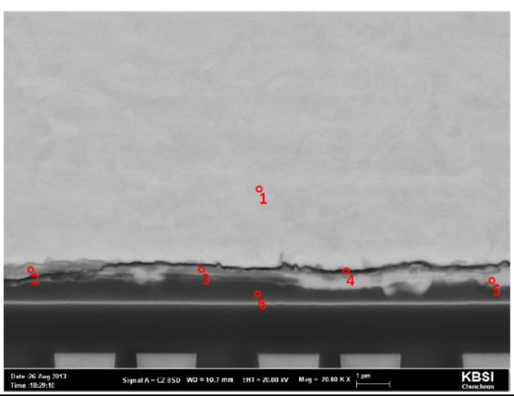

Weight%	Ag	Al	Pd	Au	O	Remark
1	95.08	-	3.14	0.36	1.42	Ag wire
2	56.84	21.68	2.39	1.26	17.84	Ag_2Al
3	67.47	21.46	2.09	0.64	8.34	Ag_2Al
4	73.79	13.69	2.07	0.41	10.03	Ag_3Al
5	59.82	26.13	0.40	-	13.65	Ag_2Al
6	29.20	54.65	0.29	1.92	13.95	Al pad

Figure 8. IMC phase of Ag-Al bond at uHAST 192h

Figure 9 showed the concentration of Cl- ions at the joint region of the wire, pad and EMC in a non-functional bond failing during uHAST for 192 h. The EDS elemental maps suggest that $Al(OH)_2Cl$ tended to form on the Al pad as a result of corrosion [20, 21].

The Cl- ions were therefore able to initiate the corrosion and accelerate the repetitive reduction and oxidation reaction which is strongly related to the failure mechanism in the Ag-Al wire bond.

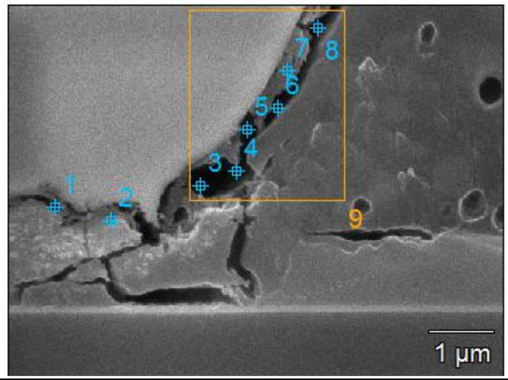

Weight%	Ag	Al	Pd	Au	O	Cl
1	72.72	8.81	3.92	1.23	12.49	0.82
2	53.28	14.47	2.24	3.91	25.32	0.78
3	43.04	29.40	0.00	0.00	20.61	6.95
4	28.93	36.25	1.31	7.27	23.70	2.53
5	43.53	20.10	1.57	4.99	26.03	3.79
6	38.92	12.87	0.04	8.46	38.42	1.29
7	33.98	6.06	1.62	13.31	44.11	0.92
8	38.12	11.56	0.00	11.54	38.09	0.70

Figure 9. EDS elemental maps at the joint region of the wire, pad and EMC

As shown in Figures 10, TEM analysis confirmed the micro-crack between Ag bonded ball and IMC layers. It could become a crack initiation point even though it was not from electrically failed unit, that is, the unit could be failed if further uHAST aging time went by. The dissolution of IMCs and the formation of Ag and Al_2O_3 due to moisture and thermal energy during uHAST could also make H_2 gas, which could cause a crack when out-gassing. The moisture control is therefore extremely important for better bonding reliability in the Ag-Al bond.

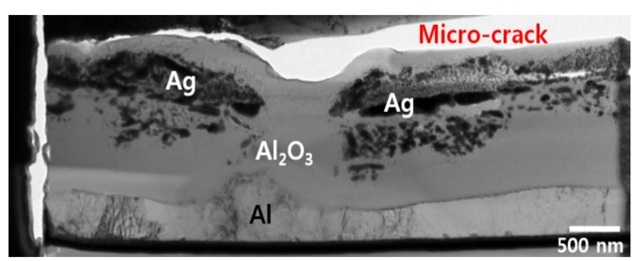

Figure 10. TEM image at uHAST 192 hours

Conclusions

We studied intermetallic compound growth and failure mechanisms to determine long term reliability of 96% silver wire bonding. To determine the IMC microstructure and failure mechanism in silver wire bonding, we analyzed the problems and found the major defect points. Summarized consideration and recommendations to discover the silver wire bonding mechanism are given below.

i) Thermal aging properties at 150°C during HTSTs showed much greater stability than those at 175°C. And more stable IMC growth was shown at Ag-Al bonds than Au-Al bonds.

ii) Influences of the mold effect on the growth rate and morphologies of the Ag/Al IMC were marginal. The type of EMC did not affect the evolution of IMCs. The IMC growth rate is about 4.46×10^{-15} at 150°C and 2.05×10^{-14} at 175°C.

iii) In HTST, micro-cracks were practically observed in the IMC after HTST, but other defects were not shown.

iv) The failure mechanism can be inferred under uHAST condition from this study. Cl- ion and moisture may cause oxidation and corrosion and finally form Al_2O_3 of insulating layer, H2 gas for crack and HCl for repetitive and accelerated reactions.

$(Ag_2Al \text{ or } Ag_3Al) + H_2O \rightarrow Al_2O_3 + Ag + H_2$

$(Ag_2Al \text{ or } Ag_3Al) + Cl^- + H_2O \rightarrow Al_2O_3 + Ag + HCl$

Acknowledgments

The STATSChipPAC Korea R&D team would like to thank Kangwon National University and Heraeus Oriental HiTec for their outstanding contribution and support toward a successful development of silver wire bonding technology.

References

1. Harman GG. Wire bonding in microelectronics - materials, processes, reliability and yield. 2nd ed. New York: McGraw-Hill; 1997.
2. Harper CA. Electronic packaging and interconnection handbook. 4th ed. New York: McGraw-Hill; 2005.
3. Prasad SK. Advanced wire bond interconnection technology. Boston: Kluwer Academic Publishers; 2004.
4. Cho JS, Jeong HS, Moon JT, Yoo SJ, Seo JS, Lee SM, et al. In: IEEE 59th Electronic components and technology conference (ECTC), San Diego; May, 2009. p. 1569.
5. Tanna S, Pisigan JL, Song WH, Halmo C, Persic J, Mayer M. In: IEEE 62nd Electronic components and technology conference (ECTC), San Diego; May-June, 2012. p. 1103.
6. Cho JS, Yoo KA, Hong SJ, Moon JT, Lee YJ, Han W, et al. In: IEEE 60th Electronic components and technology conference (ECTC), Las Vegas; June, 2010. p. 1541.
7. Chuang TH, Wang HC, Tsai CH, Chang CC, Chuang CH, Lee JD, et al. Scripta Mater 2012;67;605.
8. Tsai HH, Lee JD, Tsai CH, Wang HC, Chang CC, Chuang TH. In: IEEE 7th International Microsystems, packaging, assembly and circuits technology conference (IMPACT), Taipei; October, 2012. p. 243.
9. Chuang TH, Tsai CH, Wang HC, Chang CC, Chuang CH, Lee JD, et al. J Electron Mater 2012;41:3215.
10. Chuang TH, Chang CC, Chuang CH, Lee JD, Tsai HH. IEEE Trans Compon Packag Manuf Technol 2013;3:3.
11. Kim HG, Kim SM, Lee JY, Choi MR, Choe SH, Kim KH, et al. Acta Mater 2014;64:356.
12. Okamoto H. Phase diagrams for binary alloys. Materials Park, OH: ASM International; 2000.
13. Spencer PJ, Kubaschewski O. Monatsh Chem 1987;118:155.
14. Asta M, Johnson DD. Comput Mater Sci 1997;8:64.
15. Asta M, Hoyt JJ. Acta Mater 2000;48:1089.
16. Bozzolo g, Garcés JE, Smith RJ. Surf Sci 2005;583:229.
17. Guo R, Hang T, Mao D, Li M, Qian K, Lv Z, et al. J Alloy Compd 2014;588:622.
18. Kai LJ, Hung LY, Wu LW, Chiang MY, Jiang DS, Huang CM, et al. In: IEEE 62nd Electronic components and technology conference (ECTC), San Diego; May-June, 2012. p. 1163.
19. Cheng CH, Hsiao HL, Chu SI, Shieh YY, Sun CY, Peng C. In: IEEE 63th Electronic components and technology conference (ECTC), Las Vegas; May, 2013. p. 1569.
20. Iannuzzi M, IEEE Trans Compon Hybrids Manuf Technol 1983;6:191.
21. Paulson WM, Lorigan RP, In: IEEE 14th Annual reliability physics symposium, Las Vegas; April, 1976. P.42.